

# Synthesis and Structural Characterization of Zn(O<sub>3</sub>PCH<sub>2</sub>OH), a New Microporous Zinc Phosphonate

Gary B. Hix,<sup>\*,†</sup> Benson M. Kariuki,<sup>‡</sup> Simon Kitchin,<sup>‡</sup> and Maryjane Tremayne<sup>‡</sup>

Department of Chemistry, De Montfort University, The Gateway, Leicester LE1 9BH, U.K., and The School of Chemistry, University of Birmingham, Edgbaston, Birmingham B15 2TT, U.K.

Received August 16, 2000

Zn(O<sub>3</sub>PCH<sub>2</sub>OH) (**1**) has been formed by reaction of zinc acetate with diethyl hydroxymethylphosphonate. The acidity of the zinc solution effects hydrolysis of the phosphonate to produce phosphonic acid in situ. **1** crystallizes in the trigonal spacegroup  $R\bar{3}$ , with  $a = 15.9701(2)$  Å,  $c = 7.783(2)$  Å, and  $Z = 18$ . The compound has channels in the [001] direction, formed by phosphonate groups bridging the octahedral coordinated zinc atoms. The zinc atoms are coordinated by the three oxygens of the phosphonate group and the oxygen of the hydroxy group.

## Introduction

The desire to design new microporous materials has led to increasing interest in the synthesis of metal phosphonate materials (i.e., ones that contain [O<sub>3</sub>PR]<sup>2-</sup> or [HO<sub>3</sub>PR]<sup>-</sup>, where R is an organic group) in recent years.<sup>1,2</sup> Such materials potentially have similar applications as sorbents and catalysts as seen in traditional zeotype materials, with the added benefit that the nature of the internal surface of phosphonate materials may be altered by changing the organic functional group.

Phosphonate materials containing divalent transition metal cations are most often lamellar in nature. The metal ions are bridged by the phosphonate groups, and the remaining organic part of the acid is pendant in the interlayer region. In a majority of the lamellar materials the metal ions are octahedrally coordinated. Exceptions exist in which the metal ions are five-coordinate (trigonal bipyramidal), e.g., Cu(O<sub>3</sub>PC<sub>2</sub>H<sub>5</sub>)<sup>3</sup>, or four-coordinate (tetrahedral), e.g., Zn(O<sub>3</sub>PCH<sub>2</sub>P(O)(CH<sub>3</sub>)(C<sub>6</sub>H<sub>5</sub>))<sub>2</sub>/3H<sub>2</sub>O.<sup>4</sup>

Attempts to introduce porosity into zinc phosphonates have included using diphosphonic acids, which act as covalently bonded pillars between the layers, but this resulted in materials that are not porous.<sup>5</sup> Mixing diphosphonate and phosphate groups results in structural disorder giving rise to mesoporosity.<sup>6</sup> More recently a few microporous metal phosphonates have been reported in the literature, including some that contain zinc, e.g., β-Cu(O<sub>3</sub>PCH<sub>3</sub>),<sup>7</sup> Zn(O<sub>3</sub>PC<sub>2</sub>H<sub>4</sub>NH<sub>2</sub>),<sup>8</sup> Zn(O<sub>3</sub>PCH<sub>2</sub>CH(NH<sub>3</sub>)COO), Zn(O<sub>3</sub>PCH<sub>2</sub>CH<sub>2</sub>CH(NH<sub>3</sub>)COO),<sup>9</sup> Zn(O<sub>3</sub>P(CH<sub>2</sub>)<sub>2</sub>CO<sub>2</sub>H)·1.5H<sub>2</sub>O,<sup>10</sup> AlMePO-α,<sup>11</sup> AlMePO-β,<sup>12</sup> two uranyl phenylphosphonates,<sup>13</sup>

and Pb<sub>3</sub>(O<sub>2</sub>C(CH<sub>2</sub>)<sub>2</sub>PO<sub>3</sub>)<sub>3</sub>.<sup>14</sup> In these materials the coordination environment of the metal ion is not restricted to octahedral geometry. In the Zn materials the metal is tetrahedrally coordinated, and it is the multifunctional nature of the phosphonate groups that has resulted in the formation of extended structures. The Cu and one of the uranyl phosphonates contain five-coordinate metal ions, the other uranyl phenylphosphonate contains seven- and eight-coordinate uranium ions, and the two Al materials contain both tetrahedrally and octahedrally coordinated metal centers.

With respect to porous zinc phosphonates and to the best of our knowledge, only one material has been reported in which the Zn atoms have an exclusively octahedral coordination environment. Clearfield et al. reported the formation of a zinc phosphite Zn(HPO<sub>3</sub>H)<sub>2</sub>·3H<sub>2</sub>O (arguably a phosphonate in which R = H in the definition above) that contains a hexagonally arranged channel system (lined with H and -OH groups) and in which the Zn atoms are exclusively octahedrally coordinated.<sup>15</sup>

In several of the microporous materials mentioned above, porosity is induced because of the multifunctional nature of the phosphonic acids.<sup>8–10</sup> They are formed by cross-linking of layers or chains, and the organic part of the phosphonic acid is also involved in the coordination sphere of the metal atoms in neighboring layers (or chains). In the case of the aminophosphonate it is the nitrogen that is involved in the coordination of a neighboring Zn atom.<sup>8</sup> But in the case of the amino acid type

\* To whom correspondence should be addressed. E-mail: ghix@dmu.ac.uk. Phone: (0116) 257 7116. Fax: (0116) 257 7135.

<sup>†</sup> De Montfort University.

<sup>‡</sup> University of Birmingham.

- Clearfield, A. *Curr. Opin. Solid State Mater. Sci.* **1996**, *1*, 266.
- Clearfield, A. In *Progress in Inorganic Chemistry*; Karlin, K. D., Ed.; John Wiley & Sons, Inc.: New York, 1988; Vol. 47.
- Zhang, Y.; Clearfield, A. *Inorg. Chem.* **1992**, *31*, 2821.
- Fredoueil, F.; Penicaud, V.; Bujoli-Doeuff, M.; Bujoli, B. *Inorg. Chem.* **1997**, *36*, 4702.
- Clearfield, A. *Chem. Mater.* **1998**, *10*, 2801.
- Zhang, B.; Poojary, D. M.; Clearfield, A. *Inorg. Chem.* **1998**, *37*, 5254.
- Le Bideau, J.; Payen, C.; Palvadeau, P.; Bujoli, B. *Inorg. Chem.* **1994**, *33*, 4885.
- Drumel, S.; Janvier, P.; Deniaud, D.; Bujoli, B. *Chem. Commun.* **1995**, 1051.

- Hartman, S. J.; Todorov, E.; Cruz, C.; Sevov, S. C. *Chem. Commun.* **2000**, 1213.
- Drumel, S.; Janvier, P.; Barboux, P.; Bujoli-Doeuff, M.; Bujoli, B. *Inorg. Chem.* **1995**, *34*, 148.
- Maeda, K.; Akimoto, J.; Kiyozumi, Y.; Mizukami, F. *Angew. Chem., Int. Ed. Engl.* **1995**, *34*, 1199.
- Maeda, K.; Akimoto, J.; Kiyozumi, Y.; Mizukami, F. *Angew. Chem., Int. Ed. Engl.* **1994**, *33*, 2335. Maeda, K.; Akimoto, J.; Kiyozumi, Y.; Mizukami, F. *J. Chem. Soc., Chem. Commun.* **1995**, 1033.
- Poojary, M. D.; Grohol, D.; Clearfield, A. *Angew. Chem., Int. Ed. Engl.* **1995**, *34*, 1508. Aranda, M. A. G.; Cabeza, A.; Poojary, D. M.; Clearfield, A. *Inorg. Chem.* **1996**, *35*, 1468. Grohol, D.; Clearfield, A. *J. Am. Chem. Soc.* **1997**, *119*, 9301.
- Ayyappan, S.; Diaz de Delgado, G.; Cheetham, A. K.; Ferey, G.; Rao, C. N. R. *J. Chem. Soc., Dalton Trans.* **1999**, 2905.
- Ortiz-Avila, C. Y.; Squattrito, P. J.; Shieh, M.; Clearfield, A. *Inorg. Chem.* **1989**, *28*, 2608. Durand, J.; Cot, L.; Sghyar, M.; Rafiq, M. *Acta Crystallogr.* **1992**, *C48*, 1171.

phosphonates<sup>9</sup> and the carboxylic acid derivative,<sup>10</sup> in which the porosity arises from the cross-linking of layers, it is the carbonyl oxygen that is bonded to the metal centers.

The work of Hartman et al.<sup>9</sup> has highlighted how trifunctional phosphonic acids (counting the carboxyl and  $-\text{NH}_3$  groups of the amino acid as separate groups) can be used in the formation of pillared layered materials. In these materials the phosphonate group anchors the whole organic part to the inorganic layer and the carbonyl oxygen acts as a Lewis base and coordinates to Zn atoms in adjacent layers, thereby cross-linking them. This leaves the amine group free as a functional group within the microporous structure that might potentially be employed in a number of applications.

Metal phosphonates are usually prepared by reaction of a metal salt with a phosphonic acid, by hydrothermal methods, by refluxing appropriate solutions,<sup>16</sup> or by having metal salts make contact with molten phosphonic acids.<sup>17</sup> It is often the case, however, that the metal phosphonate is formed too rapidly to allow growth of crystals sufficiently large to allow structural determination. Phosphonic acids are formed by acid hydrolysis of dialkyl phosphonate esters, and because solutions of many metal salts are acidic, we have attempted to produce the phosphonic acid in situ, using the weak acidity of the metal salt solution to hydrolyze the phosphonate ester. This method has been reported for the syntheses of zirconium phosphonates.<sup>18</sup> In this work, the best results were obtained when a mineral acid was added to a solution containing a dialkylphosphonate ester and zirconyl chloride to effect the hydrolysis of the ester. Experiments carried out without addition of a mineral acid resulted in the formation of amorphous products.

Using the knowledge that is available concerning the formation of porous metal phosphonates and using the in situ hydrolysis of dialkylphosphonate in the synthesis procedure, we have been able to synthesize a new porous Zn phosphonate  $\text{Zn}(\text{O}_3\text{PCH}_2\text{OH})$  (**1**). This material has a channel structure and contains only octahedrally coordinated Zn atoms.

## Experimental Section

**Preparation of  $\text{Zn}(\text{O}_3\text{PCH}_2\text{OH})$ .** To a solution of 0.81 g (3.7 mmol) zinc acetate dihydrate (Aldrich) in 10 mL of distilled water was added 0.622 g (3.7 mmol) diethyl hydroxymethylphosphonate (Aldrich). This mixture was stirred for 30 min and then transferred to a Teflon lined autoclave (50% fill volume). The autoclave was then heated at 160 °C for 48 h. An amount of 0.610 g of  $\text{Zn}(\text{O}_3\text{PCH}_2\text{OH})$  (94% yield) was obtained as colorless needlelike crystals and a white polycrystalline powder, which were recovered by filtration and washed with distilled water. The crystals were subsequently used in the single-crystal analysis. (Anal. Calcd: 6.85% C; 1.72% H. Obsd: 6.99% C, 1.42% H.) PXRD and IR spectroscopy (vide infra) confirmed the polycrystalline phase to be **1**.

**X-ray Single-Crystal Measurements.** The measurements were carried out using a Rigaku R-Axis II image plate diffractometer using a rotating anode generator with  $\text{Mo K}\alpha$  radiation ( $\lambda = 0.71069 \text{ \AA}$ ). Data were collected at 23 °C. Crystals were mounted on a glass fiber using an epoxy resin. A total of 36 images covering 180° of crystal rotation were recorded. Structure solution, carried out by direct methods using the SHELXS<sup>19</sup> program within the WINGX<sup>19</sup> suite, revealed the location of all non-hydrogen atoms, which were refined anisotropically. The H atoms were located in the Fourier difference map and were

**Table 1.** Crystallographic Data for  $\text{Zn}(\text{O}_3\text{PCH}_2\text{OH})$

empirical formula	$\text{CH}_3\text{O}_4\text{PZn}$
fw	175.4
space group	$R\bar{3}$ (No. 148)
$a$ (Å)	15.970(2)
$b$ (Å)	15.970(2)
$c$ (Å)	7.783(2)
$V$ (Å <sup>3</sup> )	1719.1(4)
$Z$	18
temp (°C)	23
$\lambda$ (Å)	0.71069
$\rho_{\text{calcd}}$ (g cm <sup>-3</sup> )	3.05
$\mu$ (cm <sup>-1</sup> )	6.715
$R(F_o)^a$	0.020
$wR(F_o^2)^b$	0.051

$$^a R = \sum ||F_o| - |F_c|| / \sum |F_o|. \quad ^b wR = \{ \sum [w(F_o^2 - F_c^2)^2] / \sum [w(F_o^2)^2] \}^{1/2}.$$

subsequently refined with isotropic atomic displacement parameters. Crystallographic data for **1** is given in Table 1. A small amount of residual electron density was attributed to trapped water molecules.

**Powder X-ray Diffraction Profiles.** Data were recorded at 23 °C using Gex-monochromated  $\text{Cu K}\alpha_1$  radiation ( $\lambda = 1.54056 \text{ \AA}$ ) on a Siemens D5000 diffractometer, operating in transmission mode with a linear position sensitive detector covering 8° in  $2\theta$ . Data were collected over the range 5–55° of  $2\theta$  in steps of 0.02°. Rietveld refinement was carried out over the full data range using the GSAS program package.<sup>20</sup>

**<sup>31</sup>P NMR Measurements.** All spectra were recorded at 121.5 MHz at 25 °C on a Chemagnetics CMX-Infinity 300 spectrometer. Magic angle spinning spectra were acquired with a 3.2 mm double-resonance probe using the standard cross polarization (CP) sequence, a spinning frequency of 7.0 kHz ( $\pm 2 \text{ Hz}$ ), and a 1H coupling field strength of ca. 105 kHz. Static spectra were acquired with a 5 mm double-resonance goniometer probe using a CP spin echo sequence and a 1H decoupling field strength of ca. 50 kHz.

**TGA Measurements.** TGA experiments were carried out on a TA Instruments SDT 2960 Simultaneous DTA-TGA thermogravimetric analyzer. Samples were heated in an alumina crucible at a rate of 10 °C/min to a maximum temperature of 1200 °C in an atmosphere of flowing oxygen (100 mL min<sup>-1</sup>). Recalcined alumina was used as the reference material.

**FT-IR Measurements.** FT-IR spectra were recorded on a Nicolet 5DXC spectrometer as self-supporting KBr pellets, which typically contained about 1% mass sample.

## Results

**Structure of  $\text{Zn}(\text{O}_3\text{PCH}_2\text{OH})$  (**1**).** Positional parameters of the atoms in (**1**) are given in Table 2, and selected bond distances and angles are given in Table 3. Each Zn atom has a distorted octahedral coordination sphere (Figure 1a), with Zn–O distances in the range 1.99–2.30 Å (average 2.11 Å). The distortion of the coordination environment of Zn away from octahedral is quite pronounced; hence, a bond valence calculation (using the method of Brown and Altermatt<sup>21</sup>) was carried out. The resulting value of 2.049 shows that the Zn cation is in a good coordination sphere. The three oxygens of the phosphonate group are all bonded to Zn atoms such that two of them are shared between two metal atoms and one is directly connected to only one; this is referred to as (122) connectivity.<sup>22</sup> Two of the phosphonate

- (16) Cabeza, A.; Aranda, M. A. G.; Bruque, S.; Poojary, D. M.; Clearfield, A.; Sanz, J. *Inorg. Chem.* **1998**, *37*, 4168. Raki, L.; Detellier, C. *J. Chem. Soc., Chem. Commun.* **1996**, 2475.
- (17) Hix, G. B.; Harris, K. D. M. *J. Mater. Chem.* **1998**, *8*, 579. Hix, G. B.; Carter, V. J.; Wragg, D. S.; Morris, R. E.; Wright, P. A. *J. Mater. Chem.* **1999**, *9*, 179. Hix, G. B.; Wragg, D. S.; Bull, I.; Morris, R. E.; Wright, P. A. *J. Chem. Soc., Chem. Commun.* **1999**, 2421.
- (18) Jaffres, P.-A.; Caignaert, V.; Villemin, D. *Chem. Commun.* **1999**, 1997.

- (19) Sheldrick, G. M.; *SHELXL-97. Program for refinement of crystal structures*; University of Göttingen: Göttingen, Germany, 1997. Farrugia, L. J. *WINGX. A Windows Program for Crystal Structure Analysis*; University of Glasgow: Glasgow, U.K., 1998.
- (20) Larson, A. C.; Von Dreele, R. B. *GSAS. General Structure Analysis System*; Report No. LA-UR-86-784; Los Alamos National Laboratory: Los Alamos, NM, 1987.
- (21) Brown, D.; Altermatt, D. *Acta Crystallogr., Sect. B* **1985**, *41*, 244.
- (22) Massiot, D.; Drumel, S.; Janvier, P.; Bujoli-Doeuff, M.; Bujoli, B. *Chem. Mater.* **1997**, *9*, 6.

**Table 2.** Fractional Atomic Coordinates and Isotropic Temperature Factors (Å<sup>2</sup>) for the Atoms of Zn(O<sub>3</sub>PCH<sub>2</sub>OH)<sup>a</sup>

	<i>x/a</i>	<i>y/b</i>	<i>z/c</i>	<i>U</i> <sub>eq</sub> <sup>b</sup>
Zn(1)	0.67624(2)	0.07030(2)	0.04726(4)	0.015(1)
P(1)	0.4936(1)	0.06278(5)	0.2451(1)	0.013(1)
O(1)	0.4995(1)	0.0940(2)	0.4296(3)	0.018(1)
O(2)	0.3902(1)	0.0127(2)	0.1753(3)	0.016(1)
O(3)	0.5382(2)	-0.0017(2)	0.2118(3)	0.016(1)
O(4)	0.6102(2)	0.1520(2)	-0.0291(3)	0.020(1)
C(1)	0.5644(2)	0.1705(2)	0.1145(4)	0.020(1)
H(1)	0.524(3)	0.194(3)	0.088(5)	0.020(9)
H(2)	0.614(3)	0.220(2)	0.188(4)	0.010(8)
H(3)	0.572(4)	0.120(4)	-0.102(7)	0.05(2)

<sup>a</sup> With standard deviations in the least significant digits in parentheses. For anisotropic atoms, the equivalent isotropic temperature factors are shown <sup>b</sup>  $U_{eq} = (1/3)\sum_i \sum_j U_{ij} a_i^* a_j^* A_{ij}$ .

**Table 3.** Bond Distances (Å) and Angles (deg) for the Non-Hydrogen Atoms of Zn(O<sub>3</sub>PCH<sub>2</sub>OH)<sup>a</sup>

Zn(1)–O(1) <sup>a</sup>	1.999(3)	P(1)–O(1)	1.508(3)
Zn(1)–O(2) <sup>b</sup>	2.044(3)	P(1)–O(2)	1.530(3)
Zn(1)–O(2) <sup>c</sup>	2.116(3)	P(1)–O(3)	1.537(3)
Zn(1)–O(3) <sup>d</sup>	2.087(3)	P(1)–C(1)	1.824(4)
Zn(1)–O(3)	2.300(3)	O(4)–C(1)	1.446(4)
Zn(1)–O(4)	2.132(3)		
O(1) <sup>a</sup> –Zn(1)–O(2) <sup>c</sup>	170.7(1)	O(1) <sup>a</sup> –Zn(1)–O(2) <sup>b</sup>	98.5(1)
O(1) <sup>a</sup> –Zn(1)–O(3)	87.7(1)	O(1) <sup>a</sup> –Zn(1)–O(3) <sup>d</sup>	97.5(1)
O(1) <sup>a</sup> –Zn(1)–O(4)	87.0(1)	O(2) <sup>b</sup> –Zn(1)–O(2) <sup>c</sup>	90.8(1)
O(2) <sup>c</sup> –Zn(1)–O(3)	95.0(1)	O(2) <sup>c</sup> –Zn(1)–O(3) <sup>d</sup>	79.7(1)
O(2) <sup>c</sup> –Zn(1)–O(4)	84.7(1)	O(2) <sup>b</sup> –Zn(1)–O(3)	76.4(1)
O(2) <sup>b</sup> –Zn(1)–O(3) <sup>d</sup>	104.3(1)	O(2) <sup>b</sup> –Zn(1)–O(4)	154.9(1)
O(3) <sup>d</sup> –Zn(1)–O(3)	174.6(1)	O(3)–Zn(1)–O(4)	79.4(1)
O(3) <sup>d</sup> –Zn(1)–O(4)	99.2(1)	O(1)–P(1)–O(2)	112.6(2)
O(1)–P(1)–O(3)	114.1(2)	O(1)–P(1)–C(1)	108.2(2)
O(2)–P(1)–C(1)	107.1(2)	O(2)–P(1)–O(3)	109.3(2)
O(3)–P(1)–C(1)	105.2(2)	P(1)–C(1)–O(4)	112.1(3)

<sup>a</sup> Atoms are related by the following symmetry operators: (a)  $1/3 + x - y, 2/3 + x, 2/3 - z$ ; (b)  $2/3 + y, 1/3 - x + y, 1/3 - z$ ; (c)  $-x, -y, -z$ ; (d)  $1/3 - x + y, 2/3 - x, 2/3 + z$ .

oxygens act as bridges between infinite zigzag chains of Zn atoms, which are 3.166 Å apart, in the (001) direction (Figure 1b). Within these chains, adjacent Zn atoms are connected by an O–P–O bridge and two O bridges, forming four- and six-membered rings (in  $\beta$ -Cu(O<sub>3</sub>PCH<sub>3</sub>) the Cu atoms are connected only by O bridges, thereby forming four-membered rings).<sup>5</sup> The chains are then cross-linked by O–P–O and P–C–O–Zn bridges, thus forming hexagonal channels parallel to the *c* axis, which have a diameter of 5.68 Å between two opposite methylene carbons (3.787 Å between methylene hydrogens directed into the channel) (Figure 2). The remaining coordination site of the Zn atom is occupied by the O of the hydroxy group, O4, of the phosphonate moiety. Hence, the functional group is bound to the inorganic part of the framework rather than directed into the channels, as observed in  $\beta$ -Cu(O<sub>3</sub>PCH<sub>3</sub>).<sup>7</sup> The hydroxyl oxygen, O4, also hydrogen-bonds to O3, with the O3–O4 distance being 2.76 Å and the O–H–O angle being 152.9°.

Rietveld refinement of the structural model against powder X-ray diffraction data confirms the structure of **1** and verifies that the as-made sample contains only one crystalline phase (Figure 3).

**Infrared Spectroscopy.** The IR spectrum of **1** exhibits broad peaks at 3430, 3232, and 1633 cm<sup>-1</sup> that arise from the stretching and bending modes of the hydrogen-bonded hydroxyl groups present within the channel. The reduction in the frequency with respect to the expected frequency arises from the fact that the oxygen is coordinated to Zn, thereby slightly reducing the strength of the O–H bond. The stretching bands

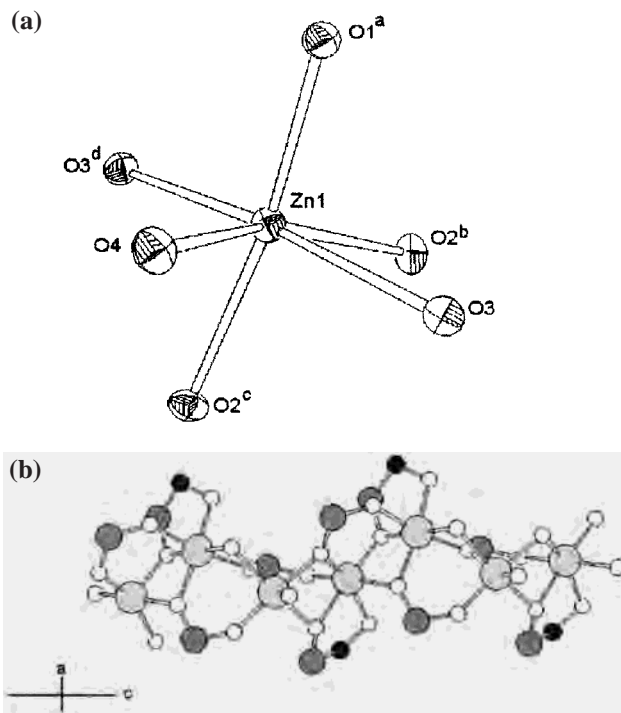


**Figure 1.** (a) ORTEP diagram (50% probability ellipsoids) showing the coordination of Zn in Zn(O<sub>3</sub>PCH<sub>2</sub>OH) (**1**). Atoms related by the following symmetry operators: (a)  $1/3 + x - y, 2/3 + x, 2/3 - z$ ; (b)  $2/3 + y, 1/3 - x + y, 1/3 - z$ ; (c)  $-x, -y, -z$ ; (d)  $1/3 - x + y, 2/3 - x, 2/3 + z$ . (b) Ball-and-stick diagram showing the zinc phosphonate chains running in the (001) direction. Zn atoms are shown as large light-gray spheres, P atoms as dark-gray spheres, C atoms as filled spheres, and O atoms as open spheres.

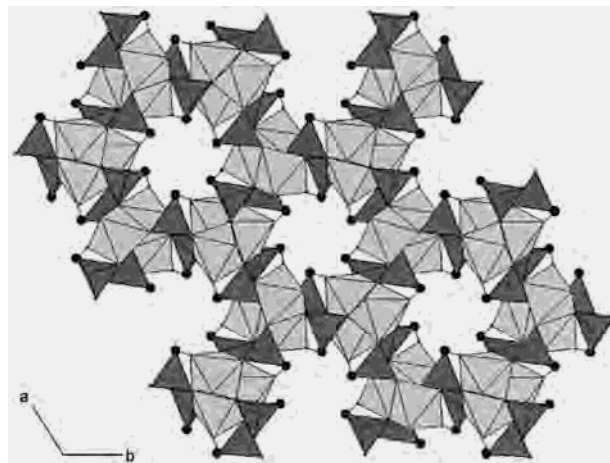


**Figure 2.** Polyhedral view of the structure of **1** showing the channels running parallel to the (001) direction. The ZnO<sub>6</sub> octahedra and the O<sub>3</sub>PC tetrahedra are shown as light- and dark-gray polyhedra, respectively.

of the methylene group are seen at 2996, 2948, and 2809 cm<sup>-1</sup>. The P–C stretching mode is observed as a sharp peak at 1438 cm<sup>-1</sup>, and the P–O stretching modes are seen as a number of sharp peaks in the range 1150–950 cm<sup>-1</sup>.

**<sup>31</sup>P NMR Spectroscopy.** The <sup>31</sup>P MAS NMR and static spectra of **1** are shown in Figure 4. The MAS spectrum (Figure 4a) exhibits a peak at 18.8 ppm, which is in agreement with that obtained by fitting the static spectrum (Figure 4b, Table 4). The observed isotropic chemical shift is somewhat upfield from that expected according to the work of Massiot et al. (vide infra).<sup>22</sup> The peak is seen to be slightly asymmetric, which probably results from some disorder (static or ultraslow



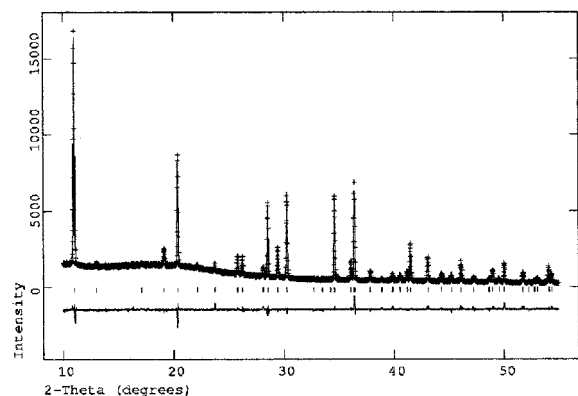


**Figure 3.** Final observed (crosses), calculated (solid line), and difference plots for the Rietveld refinement against powder diffraction data for **1**.

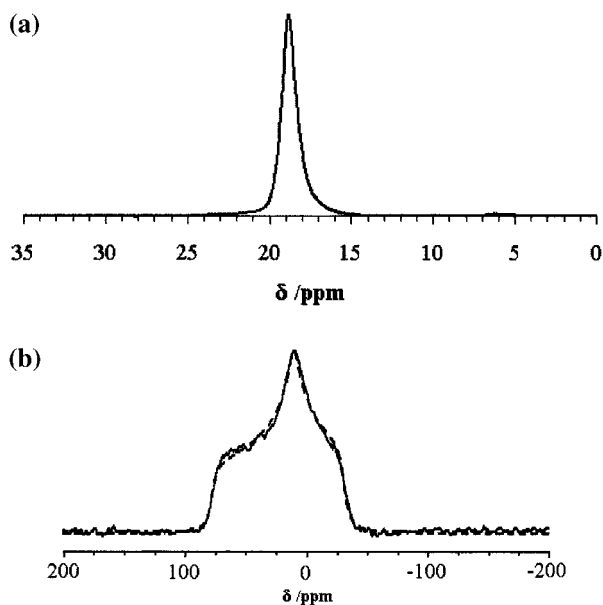


**Figure 4.** (a)  $^{31}\text{P}$  MAS NMR spectrum and (b) the  $^{31}\text{P}$  static spectrum of **1**. The solid line represents the observed spectrum, and the dashed line represents the fit obtained using the parameters given in Table 4.

**Table 4.**  $^{31}\text{P}$  Chemical Shift Tensor Data for  $\text{Zn}(\text{O}_3\text{PCH}_2\text{OH})$  Compared with Literature Values for Materials with the (122) Connectivity<sup>18</sup>

compound	$\delta_{\text{iso}}^a$ , ppm	$\eta^b$	$\Delta^c$	$\delta_{11}$ , ppm	$\delta_{22}$ , ppm	$\delta_{33}$ , ppm
$\text{Zn}(\text{O}_3\text{PCH}_2\text{OH})$	18.8	0.7	59.0	-31.4	10.0	77.8
$\text{Zn}_3(\text{O}_3\text{PC}_2\text{H}_4\text{CO}_2)_2$	35.9	0.9	-33.8	68.0	37.6	2.1
$\text{Zn}(\text{O}_3\text{PC}_2\text{H}_4\text{CO}_2\text{H})\cdot\text{H}_2\text{O}$	38.1	0.9	-38.2	73.5	41.0	-0.1
$\text{Zn}(\text{O}_3\text{PC}_2\text{H}_5)\cdot\text{H}_2\text{O}$	37.7	0.9	-35.8	71.7	39.5	1.9

<sup>a</sup> All values are given relative to 85%  $\text{H}_3\text{PO}_4$ . <sup>b</sup> Chemical shift asymmetry is defined as  $|\delta_{22} - \delta_{11}|/|\delta_{33} - \delta_{\text{iso}}|$  with the convention of Haeberlen.<sup>23</sup> <sup>c</sup> Chemical shift anisotropy is defined as  $\delta_{33} - \delta_{\text{iso}}$ .

dynamic) of the P environment. It is thought that the residual electron density, assigned as being a small quantity of trapped water, causes a small distribution of the P sites observed as a slightly asymmetric peak. There is an additional peak at 6.3 ppm, which is very small and is thought to indicate the presence of a very small quantity of an impurity phase; this phase was not observed in the powder X-ray diffraction studies.

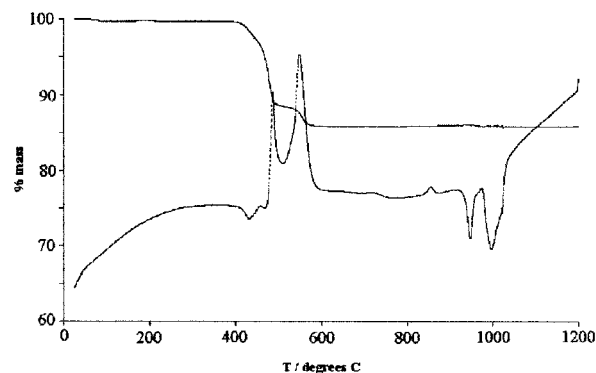


**Figure 5.** TGA and DTA traces for **1** heated in  $\text{O}_2$  from room temperature to 1200 °C.

**Thermogravimetric and CHN Analysis.** The TGA trace for **1** shows two stepwise mass losses (Figure 5) and a total mass loss upon heating to 1200 °C in flowing oxygen of 14.19%, which is consistent with the formation of  $\text{Zn}_2\text{P}_2\text{O}_7$  following loss of the organic part of the material (calculated mass loss is 14.14%). This value is also consistent with the CHN analyses. The TGA trace shows an initial very small mass loss (<1%) below 100 °C, attributed to loss of the trapped water molecules located within the channels. The second mass loss, centered at 486 °C, is thought to result from an initial condensation of the hydroxyl groups, and resultant loss of water, followed by the oxidation of the hydrocarbon part of the phosphonate group at around 550 °C.

## Discussion

The syntheses of metal phosphonates directly from the relevant dialkylphosphonate appear to be an extremely productive adaptation of the traditional hydrothermal methods employed in the syntheses of these materials. The metal salt solution is sufficiently acidic to carry out the hydrolysis of the phosphonate to produce the phosphonic acid in situ without having to introduce additional mineral acids.

The use of this method has a benefit in the syntheses of metal phosphonates. First, use of the phosphonate ester rather than the phosphonic acid removes the need to synthesize the acid. Because dialkylphosphonates are often far easier to purify (this can often be achieved by simple distillation procedures) than the corresponding phosphonic acids, a possible source of impurity and a step in the overall synthesis procedure have been removed.

We are currently investigating the application of this procedure in the syntheses of phosphonates containing more complex organic functional groups.

All but three of the previous examples of zinc phosphonates reported in the literature have been lamellar in nature. In the layered materials, the zinc atom often has an octahedral coordination environment. In  $\text{Zn}(\text{O}_3\text{PC}_2\text{H}_4\text{NH}_2)$ ,<sup>8</sup>  $\text{Zn}(\text{O}_3\text{PCH}_2\text{CH}(\text{NH}_3)\text{COO})$ , and  $\text{Zn}(\text{O}_3\text{PCH}_2\text{CH}_2\text{CH}(\text{NH}_3)\text{COO})$ ,<sup>9</sup> the only previously reported zinc phosphonates with channel structures, the zinc atoms are four-coordinate. Zinc hydroxymethylphosphonate, reported here, contains Zn in an exclusively octahedral coordination environment. The structure is very similar to that of a zinc phosphite  $\text{Zn}(\text{HPO}_3\text{H})_2\cdot\frac{1}{3}\text{H}_2\text{O}$ ,<sup>15</sup> which contains a similar channel structure in which Zn is octahedrally coordinated and the hexagonal channels are lined with P-H and P-OH groups. The main difference between the structures is the size of the channels, the channels in the phosphite being larger at 7.53 Å. This is almost certainly a consequence of the difference

(23) Haeberlen, U. *High Resolution NMR in Solids: Selected Averaging; Advances in Magnetic Resonance*, Supplement 1; Academic Press: New York, 1976; p 9.

in stoichiometry of the two materials; because the phosphite groups only carry a single negative charge, there are two phosphite groups per Zn atom, as opposed to only one phosphonate group per zinc atom in the hydroxymethylphosphonate. The size of the roughly circular channels in **1** (approximate diameter 3.8 Å) is closer to that reported for Zn(O<sub>3</sub>PC<sub>2</sub>H<sub>4</sub>NH<sub>2</sub>), which contains elliptical channels of dimensions 3.6 Å × 5.3 Å.

It has already been noted by Bujoli et al. that the use of a functionalized phosphonic acid can clearly act as an efficient building block for the syntheses of open-framework three-dimensional materials.<sup>7</sup> In several examples reported in the literature, the metal coordination sphere is completed by the functional group at the end of the phosphonate. It would appear that the use of bifunctional phosphonates is instrumental in the preparation of porous materials of this type. The material reported here reiterates this point, and we are in the process of investigating similar systems that might lead to the syntheses of new microporous materials.

This type of “double coordination” has been observed in a number of other materials. Though this undoubtedly stabilizes the three-dimensional nature of the material, it does mean that the functional group may no longer be available for catalysis or coordination, and it is only where trifunctional phosphonic acids are used that a functional group might end up in a situation where it might usefully be employed.<sup>10</sup> A similar approach has been demonstrated to be successful in the syntheses of functionalized zirconium diphosphonates.<sup>24</sup> The use of  $\alpha,\omega$ -polyimine and polyether diphosphonates results in the inclusion of active functional groups and cross-linking of the zirconium layers.

(24) Ortiz-Avila, C. Y.; Clearfield, A. *Inorg. Chem.* **1985**, *24*, 1773. Ortiz-Avila, C. Y.; Bhardwaj, C.; Clearfield, A. *Inorg. Chem.* **1994**, *33*, 2499.

A <sup>31</sup>P MAS NMR spectroscopic study of other zinc phosphonates has shown that, in general, observed isotropic chemical shifts,  $\delta_{\text{iso}}$ , move downfield as the connectivity increases.<sup>22</sup> The chemical shift of the isotropic peak in the <sup>31</sup>P NMR spectrum of **1** ( $\delta = 18.8$  ppm) is much further upfield from the value expected given the connectivity (122) of the phosphonate group. In fact, the observed  $\delta_{\text{iso}}$  is further upfield than other materials in which the phosphonate has a connectivity of (111).<sup>22</sup> The observed isotropic shift was verified by analysis of the static <sup>31</sup>P solid-state NMR spectrum (Figure 4b); the parameters derived from this spectrum are compared to those obtained from the spectra of materials with the same connectivity in Table 4. This behavior is observed because in **1** the isotropic chemical shift is strongly affected by the coordinating hydroxyl group. In phosphonates based on 2-carboxyethylphosphonic and 2-aminoethylphosphonic acids, the functional group is separated from the P center and the chemical shift is dependent only on PO<sub>3</sub> connectivity.

In summary, making phosphonate materials directly from the dialkylphosphonates simplifies the synthesis procedure and we have used it to synthesize a microporous zinc phosphonate. We have demonstrated that the use of this method in conjunction with phosphonates that are multifunctional, thereby yielding porous materials (with or without additional available functional groups), puts us one step closer to the goal of materials chemists to be able to synthesize, at will, materials that are designed to fulfill a specific chemical role.

**Acknowledgment.** The authors thank Mrs. N. Garrington for collecting the IR data. M.T. thanks the Royal Society for provision of a University Research Fellowship.

**Supporting Information Available:** Crystallographic file, in CIF format. This material is available free of charge via the Internet at <http://pubs.acs.org>.

IC000943X